

Myosin V is a left-handed spiral motor on the right-handed actin helix

M. Yusuf Ali¹⁻³, Sotaro Uemura⁴, Kengo Adachi^{1,2}, Hiroyasu Itoh^{2,5}, Kazuhiko Kinoshita Jr¹⁻³ and Shin'ichi Ishiwata^{2,4}

¹Center for Integrative Bioscience, Okazaki National Research Institutes, Higashiyama 5-1, Myodaiji, Okazaki 444-8585, Japan. ²CREST (Core Research for Evolutional Science and Technology), 'Genetic Programming' Team 13, Nogawa 907, Miyamae-ku, Kawasaki 216-0001, Japan.

³Department of Physics, Faculty of Science and Technology, Keio University, Hiyoshi 3-14-1, Kohoku-ku, Yokohama 223-8522, Japan. ⁴Department of Physics, School of Science and Engineering, Waseda University, Okubo 3-4-1, Shinjuku-ku, Tokyo 169-8555, Japan. ⁵Tsukuba Research Laboratory, Hamamatsu Photonics KK, Tokodai, Tsukuba 300-2635, Japan.

Published online: 13 May 2002, DOI: 10.1038/nsb803

Myosin V is a two-headed, actin-based molecular motor implicated in organelle transport. Previously, a single myosin V molecule has been shown to move processively along an actin filament in discrete ~36 nm steps. However, 36 nm is the helical repeat length of actin, and the geometry of the previous experiments may have forced the heads to bind to, or halt at, sites on one side of actin that are separated by 36 nm. To observe unconstrained motion, we suspended an actin filament in solution and attached a single myosin V molecule carrying a bead duplex. The duplex moved as a left-handed spiral around the filament, disregarding the right-handed actin helix. Our results indicate a stepwise walking mechanism in which myosin V positions and orients the unbound head such that the head will land at the 11th or 13th actin subunit on the opposing strand of the actin double helix.

Class V myosin has two globular motor domains that interact with an actin filament to generate force upon ATP hydrolysis; the motor supports a wide variety of cellular movements¹⁻⁵. Myosin V consists of two identical heavy chains, each composed of an N-terminal motor domain ('head'), six IQ motifs that bind light chains ('neck'), a coiled coil tail domain and a globular cargo-binding domain¹. A single myosin V molecule moves along an actin filament for many catalytic cycles without dissociating from the filament⁶⁻⁸. Steps of ~36 nm have been identified in this processive movement^{6,7,9}, and the two heads of myosin V have been shown to bind to actin ~36 nm apart¹⁰, suggesting that myosin V 'walks' on actin with 36 nm strides by alternate binding of the two heads.

Whether myosin V really walks and, if so, how its step size is determined are fundamental issues relating to the motor mechanism. The step size measurements above were made either with myosin V fixed on a surface^{6,9} or actin filaments lying on a surface^{7,10} such that myosin V could approach an actin filament only from one side. Myosin V had to move straight on actin; thus, the motor may well have been forced to step on blue actin subunits (Fig. 1a), which are 36 nm apart. Here we allow myosin V to freely rotate around an actin filament and monitor how or whether the motor walks. If myosin V walks but its natural step size is slightly longer or shorter than 36 nm, unconstrained motion should be a right- or left-handed, long-pitch spiral.

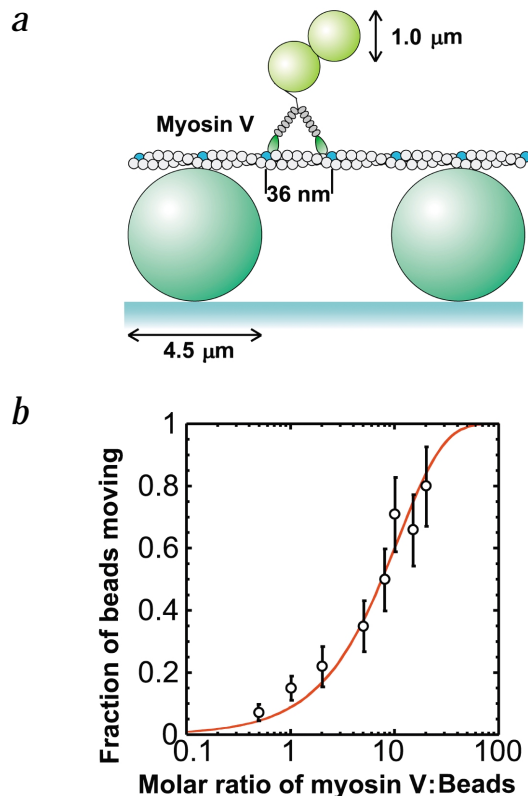


Fig. 1 Experimental design. **a**, Motility assay system (not to scale). The heads of myosin V are green; the necks, gray. Every 13th actin subunit is blue. **b**, Fraction of beads that moved more than ~0.5 μm along an actin filament (see Methods). Error bars indicate $\pm n^{1/2} N^{-1}$, where n is the number of beads that moved and N (50 or 100) is the number of trials. Line shows the theoretical probability that a bead carries one or more active motors, $1 - \exp(-\lambda c)$, where c is the molar ratio of myosin V to beads and λ (0.092) is the fit parameter³⁰.

Alternatively, steps may be so short that myosin V sequentially interacts with neighboring actin subunits in one of the two helical strands (crossing onto the other strand would require extremely 'bowlegged' necks). In this case, myosin V would undergo extensive right-handed rotation, as does RNA polymerase around DNA¹¹. A single head might glide over many actin subunits in a strand during one ATPase cycle¹². Such gliding is not necessarily inconsistent with the observed ~36 nm steps, because gliding would be forced to stop at ~36 nm when rotation around the actin filament is prohibited. Direct observation of rotation will distinguish between these cases.

Myosin V rotates as a left-handed screw

To allow myosin V to freely rotate around an actin filament, we suspended an actin filament between two large (4.5 μm) beads immobilized on a glass surface¹³ (Fig. 1a); a similar system has been reported¹⁴. Using optical tweezers, we positioned a duplex of smaller (1 μm) beads that were pre-incubated with myosin V at the molar ratio of 1:1 onto the midpoint of the filament. When the laser trap was turned off, the duplex started to move along and, at the same time, rotate around the actin filament. Results from experiments in which single 1 μm beads prepared at various myosin:bead ratios were allowed to move along an actin filament (Fig. 1b) indicate that a single myosin V molecule is most likely responsible for this motion. The fraction of moving beads as a function of myosin:bead ratio fit well to a

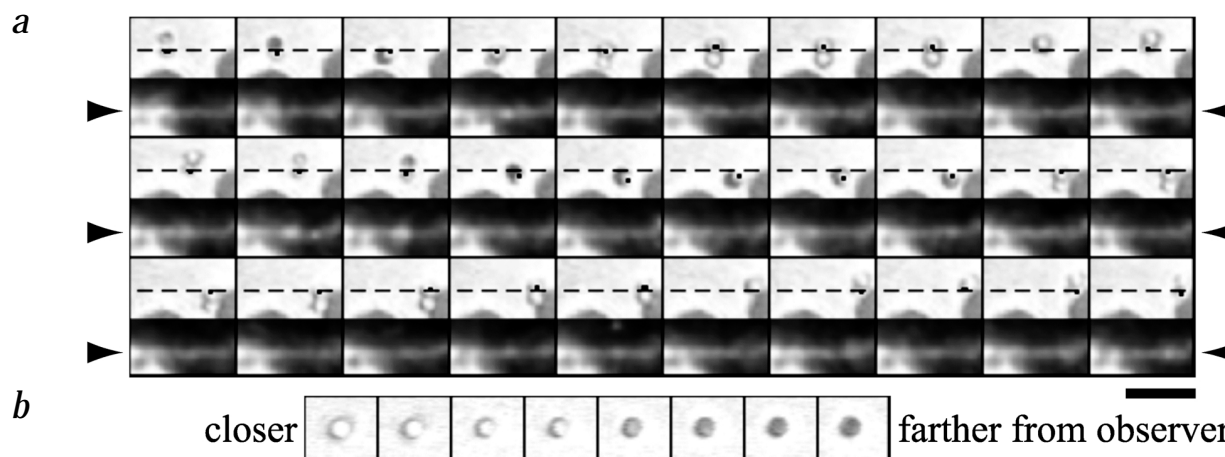


Fig. 2 Spiral motion of myosin V around an actin filament at 400 μM ATP. **a**, Sequential images at 1 s intervals. Upper and lower panels show bright-field and corresponding fluorescence images, respectively. The bar corresponds to 5 μm . Dashed lines are the position of the actin filament deduced from lower panels (arrow heads); dots, center of the beads that are judged to be on actin. Note that the actin filament remained straight. **b**, Images of a 1 μm bead at decreasing heights (left to right at $-0.2 \mu\text{m}$ intervals) from the glass surface. Because our images represent views from above the sample²⁷, white beads in (a) and (b) are closer to the observer, whereas the black beads are farther away.

Poisson distribution (solid line); this fit indicates that >95% of moving beads were driven by only one myosin V molecule. These single beads also rotated around the actin filament, but precise analysis was far easier with the bead duplex.

Myosin V-decorated bead duplexes were allowed to move along an actin filament at 400 μM ATP, where the linear velocity of the motor was maximal. Sequential video images of such a system reveal that the bead duplex rotates around the actin filament (Fig. 2a; movies at <http://k2.ims.ac.jp>). In these images, a bead that appears white is closer to the observer, whereas a black one is farther from the observer (Fig. 2b). Thus, the duplex moved as a left-handed screw, making two revolutions while traveling over $\sim 4.4 \mu\text{m}$. Such complete rotations were observed at all ATP concentrations examined, and all complete rotations were left-handed. This is in contrast to myosin II, which rotates as a right-handed screw¹⁵. Not all bead duplexes bound to an actin filament showed clear rotation (Table 1), the primary reasons being either that they did not move long enough or the filament was $<2 \mu\text{m}$ from the surface. There were 10 instances where, with no apparent reason, the duplex moved for $>1 \mu\text{m}$ without appreciable rotation (Fig. 3c; Table 1). Presumably, the filament height was $\sim 2 \mu\text{m}$ or some debris was attached to the duplex and impeded rotation. Indeed, we occasionally observed beads carrying relatively large debris, including short actin fila-

ments, in the fluorescence image. Smaller debris would have been unnoticed. That myosin V can move without rotation is consistent with the previous observations of stepping on actin lying on a surface.

Unconstrained step size is 34.8 nm

From the time courses of rotation and displacement along actin for individual bead duplexes (Fig. 3a–c), we determined the relation between rotation and displacement for all duplexes that made >1 revolution (solid lines in Fig. 3d). All of these curves (Fig. 3d) are within a narrow zone, showing that the rotation and displacement are well correlated, except for the presumably impeded cases (Fig. 3c, dotted lines in Fig. 3d). Myosin V travels a distance of $2.2 \pm 0.3 \mu\text{m}$ per one left-handed revolution (mean \pm s.d. for linear fits to 22 solid curves in Fig. 3d), which is constant over ATP concentrations from 1 μM to 1 mM, where the linear velocity of the motor changes from 5 to 320 nm s^{-1} .

The left-handed rotation of single myosin V molecules indicates a step size slightly smaller than the actin helical repeat of 36 nm (Fig. 4). Steps shorter than 18 nm, including the case of sliding along one helical strand¹², would result in right-handed rotation. Because the difference between the helical repeat of actin and the step size of myosin V motor (blue/cyan *versus* red in Fig. 4) must add up to one full turn of actin helix (72 nm) over the travel distance of 2.2 μm , the average step size is given by $36 \text{ nm} \times (2,200 \text{ nm} - 72 \text{ nm}) / (2,200 \text{ nm}) = 34.8 \text{ nm}$. This number derived from the actin repeat is rather precise ($\pm 0.1 \text{ nm}$) and is insensitive to the uncertainty in the 2,200 nm value. On average, myosin V rotates 6° ($360^\circ \times 34.8 \text{ nm} / 2,200 \text{ nm}$) per step left around the actin filament.

Step size is constant

The step size of 34.8 nm above is the one at no load. Hydrodynamic friction against the bead duplex is given by $2 \times 6\pi\eta av$, where η ($0.001 \text{ N m}^{-2} \text{ s}$) is the viscosity of water; a ($0.5 \mu\text{m}$), the bead radius; and v ($<320 \text{ nm s}^{-1}$), the bead velocity. Thus, the frictional load is at most 0.006 pN, far less than the maximal pulling force, 3 pN, produced by a single myosin V molecule⁶. The frictional torque against rotation is given by¹⁶: $(2 \times 8\pi\eta a^3 + 6\pi\eta a^3 + 6\pi\eta a^2)r\omega$, where r is the distance between

Table 1 Summary of bead duplex experiments at 1:1 myosin V:bead

Total number of bead duplexes tested at	
1–1,000 μM ATP	1,040
Duplexes bound to actin	229
Active duplexes ¹	156 (100%)
Moved only for $<1 \mu\text{m}$	57 (37%) ²
Moved for $>1 \mu\text{m}$ and made >0.5 revolution	43 (28%)
Moved for $>1 \mu\text{m}$ without rotation ³	46 (29%)
Moved for $>1 \mu\text{m}$ without rotation ⁴	10 (6%)

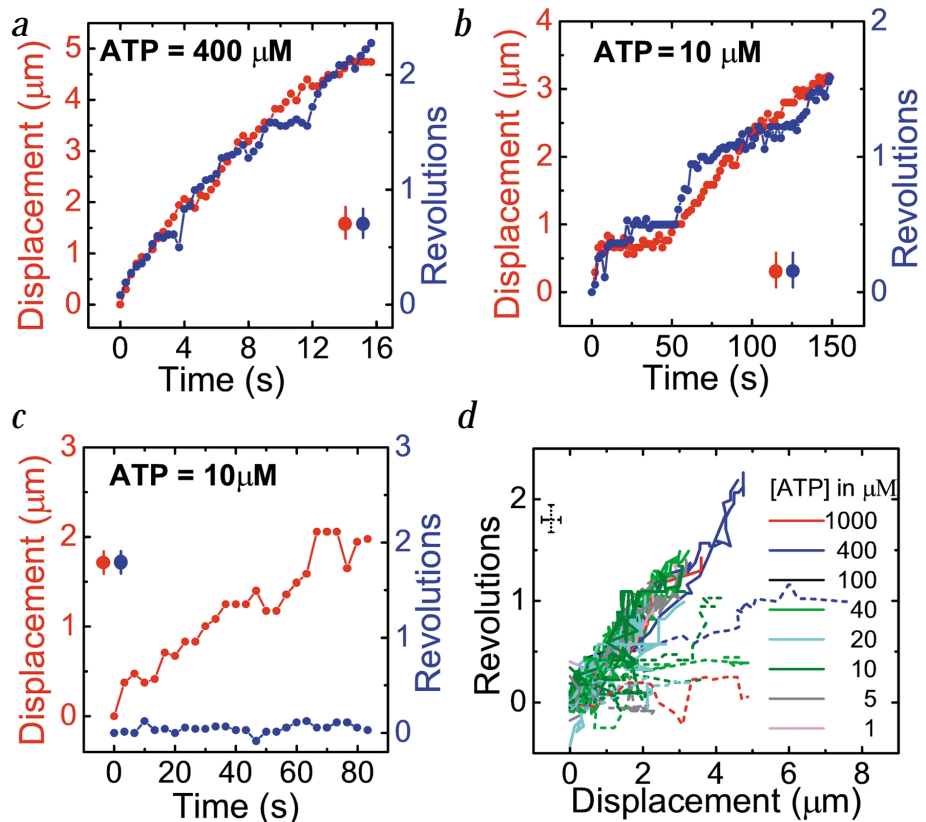
¹Defined as having moved along actin for $>0.5 \mu\text{m}$.

²Actin filaments were not long enough in 22 cases.

³The filament height was $<2 \mu\text{m}$.

⁴Reason for no rotation is unknown.

Fig. 3 Correlations between displacement and rotation. **a, b.** Typical time courses. Error bars are likely uncertainties in human judgment (see Methods). **c.** A case of linear motion. **d.** Relationship between sliding distance and rotation. ATP concentrations are distinguished by color and indicated in μM . Dashed lines represent linear motion or irregular rotation.



the center of the outer bead and actin filament, and ω is the angular velocity. A duplex with $r = 1.2 \mu\text{m}$ was found to rotate at $\omega = 0.9 \text{ radian s}^{-1}$, giving the highest torque of 20 pN nm , and several other duplexes showed the torque at $>10 \text{ pN nm}$. These values are apparently quite high, comparable to the 40 pN nm of torque produced by the rotary molecular motor $F_1\text{ATPase}^{17}$. In one step, however, myosin V rotates only $6^\circ = 0.1 \text{ radian}$; thus, the work done for rotation is at most 2 pN nm ($20 \text{ pN nm} \times 0.1 \text{ radian}$), only half the thermal energy. The frictional torque is completely negligible at low ATP concentrations.

The step size of myosin V is $\sim 35 \text{ nm}$ under a variety of conditions. Duplexes prepared at 10^4 myosin V molecules per bead also made one left-handed rotation per $2.5 \pm 0.5 \mu\text{m}$ at $40 \mu\text{M}$ ATP ($n = 8$). This is a loaded condition, because a stepping myosin V molecule has to work against others that are simultaneously bound to actin. Consistent with this, a step size of 35 nm has recently been reported⁹ under a load of 1 pN . Load independence of the step size may imply that myosin V does not readily fluctuate toward right or left when it stands on one foot ('head'). To determine if myosin V tends to interact with intervening actin subunits during the long strides, we examined bead motions at increasing ionic strengths, which would result in diminished actin–myosin interaction¹⁸. The average distances traveled at 50, 100, 200 and 300 mM KCl were 2.1, 2.1, 1.5 and $1.1 \mu\text{m}$ ($n = 8, 23, 7$ and 7), respectively, indicating reduction in processivity as expected. Rotations, however, were all left-handed and one revolution per $2.3 \pm 0.5 \mu\text{m}$ at all ionic strengths. Myosin V seems to stride over intervening actin subunits.

Discussion

Spiral motion of a single motor molecule around a helical track should reveal how the motor successively interacts with the repeating units composing the track. To our knowledge, myosin V is the first example of a processive motor spiraling with a pitch incommensurate to the helical pitch of the track; kinesin¹⁹ and RNA polymerase¹¹ precisely follow their respective helical track. The deduced step size of 34.8 nm for myosin V is much larger than the intersubunit distance of 5.5 nm in one strand of the actin filament, indicating that myosin V walks with long strides; sliding along one strand of actin helix¹² is unlikely.

There are 13 actin subunits per 36 nm , counting both strands. Our results indicate that, during unconstrained walking, myosin V aims at the 11th (red, Fig. 4) or 13th (blue) actin subunit on the opposing strand (binding to the 12th subunit on the opposite side of the filament would be sterically hindered). This almost straight walking is not a trivial task, because, unlike a human, the two feet ('heads') of myosin V are identical and related by basic two-fold symmetry. Landing on the 13th subunit would require 180° twist of the neck from its symmetry-related orientation. Although the twist would imply extensive flexibility in the neck (and/or head), a proper posture of the bound head and neck is to aim at a correct target among identical actin subunits in the double helix. Recent reports^{20,21} suggest that $\sim 25 \text{ nm}$ of the step size of $\sim 35 \text{ nm}$ is accounted for by the swing of the bound neck and the rest by diffusion of the unbound head. The swing, then, must be a delicate combination of bending and twisting that ensures diffusional landing on, mostly, the 11th or 13th subunit, irrespective of load.

The natural way of walking is one in which the two heads move forward alternately²². Alternate binding of two identical heads should result in 180° rotation of the entire molecule

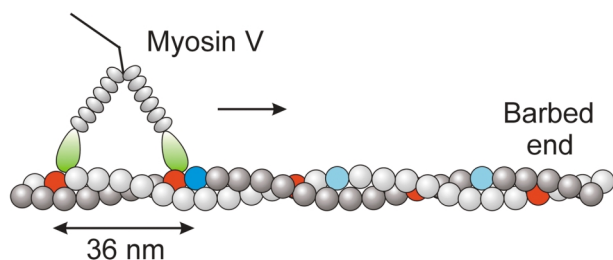


Fig. 4 Interpretation of the left-handed rotation. Stepping on every 11th actin subunit (red) would result in left-handed spiral movement, whereas linear movement is expected on the 13th subunits (blue/cyan). The estimated step size of 34.8 nm is between the 11th and 13th subunits.

around its symmetry axis every time the motor steps²², but kinesin failed to show this²³. We examined whether our bead duplex would rotate around the point of attachment to actin at low concentrations of ATP (500 nM–1 μ M), but, similar to kinesin, we have seen no convincing evidence of 180° rotation. This is apparently inconsistent with simple walking, although oblique attachment of myosin V to the bead surface may have impeded the rotation of the bead duplex. Simple walking has also been challenged by recent findings: myosin VI^{9,24} and mutated myosin V¹², both short necked, made large steps apparently incompatible with the head and neck sizes. Conformational changes, or melting, in the head/neck region would be required to allow a long stride, as in kinesin²⁵. Whether, or in which direction, these short-necked myosins rotate remains to be seen.

Methods

Sample preparation. Myosin V was purified from chick brain²⁶. Rabbit skeletal actin was biotinylated and stained with phalloidin-tetramethylrhodamine essentially as described²⁷ but without crosslinking; the molar ratio of actin to biotin-PE-maleimide was 1:2. Polystyrene beads (1 μ m, F-8814, Molecular Probes) were incubated for 30 min in buffer A (10 mM imidazole, pH 7.6, 100 mM KCl, 4 mM MgCl₂, 1 mM EGTA and 5 mM dithiothreitol (DTT)) containing 10 mg ml⁻¹ BSA and centrifuged for 15 min at 18,000 \times *g*. Of the beads, ~10% formed duplexes. The beads were coated with myosin V as described⁷. To assess the coating efficiency (Fig. 1b), a single bead was selected and held in an optical trap²⁸ near an actin filament suspended in buffer A containing 1 mM ATP (see below). Then, the filament was moved across the bead in various directions by moving the microscope stage until the bead attached to the filament. If attachment did not occur within ~1 min, the bead was repositioned and the manipulation was repeated several times. After attachment, the trap was turned off to allow movement of the bead along actin. The fraction of beads that were bound but did not move >–0.5 μ m was <–0.1 (0.03 at the myosin/bead ratio, *c*, of 0.5 and 0.09 at *c* = 1). The motility assay below was done on duplex beads prepared at *c* = 1, unless stated otherwise.

Motility assay. Carboxylated polystyrene beads (4.5 μ m; Polyscience) were amino-derivatized and biotinylated²⁹. The beads were incubated with 10 mg ml⁻¹ streptavidin, washed and infused in a flow chamber. After 10 min, 5 mg ml⁻¹ BSA was infused and incubated for 1 min. Biotinylated and labeled actin filaments were infused and allowed to bind to the 4.5 μ m beads to form actin bridges. Then, 0.25–1 pM of beads decorated with myosin V in buffer A containing ATP, 6 mg ml⁻¹ glucose, 0.2 mg ml⁻¹ glucose oxidase, 0.02 mg ml⁻¹ catalase and 0.2% β -mercaptoethanol were infused into the flow cell. To minimize Brownian motion, only tightly suspended actin filaments were used. If such a filament was not found, we moved the 4.5 μ m beads with the optical tweezers to form a tight actin bridge. Torsional Brownian motion of actin is <±50° for a 10 μ m filament¹³. Finally, we positioned a bead duplex onto an actin filament using the optical tweezers, moved the filament until it bound the duplex and turned off the optical trap to let

the duplex move along the actin filament. If unsuccessful, this maneuver was repeated 10–30 \times . The microscope system has been described²⁸; bright-field images showing bead movement and fluorescence images showing actin filaments were simultaneously recorded with video cameras. Positions and orientations of bead duplexes were analyzed by eye to the precision of \pm 0.5 μ m and \pm 0.25 revolutions. For the orientation, video images were compared with pairs of overlapping circles representing views of two spheres at known angles. Because of drift in the microscope focus, there were rare occasions where distinction between the two beads became difficult; large deviations from linear relationship in Fig. 3d, seen in some curves, may be due to human error. Observations were made at 23 °C.

Acknowledgments

We thank R. Yasuda, H. Noji, T. Nishizaka, Y. Harada and T. Nishinaka for discussion; L.B. Roksana, K. Kawashima, K. Yogo, R. Shimo, J. Yamaguchi and H. Kubota for sample preparation; M. Shio for microscope setup and H. Umezawa for laboratory management. M.Y.A. was a research fellow of the Japan Society for the Promotion of Science. This work was supported in part by Grants-in-Aid from the Ministry of Education, Culture, Sports, Science, and Technology of Japan.

Competing interests statement

The authors declare that they have no competing financial interests.

Correspondence should be addressed to K.K. email: kazuhiko@ims.ac.jp

Received 7 March, 2002; accepted 16 April, 2002.

- Cheney, R.E. *et al.* *Cell* **75**, 13–23 (1993).
- Mermall, V., Post, P.L. & Mooseker, M.S. *Science* **279**, 527–533 (1998).
- Rogers, S.L. & Gelfand, V.I. *Curr. Biol.* **8**, 161–164 (1998).
- Tabb, J.S., Molyneaux, B.J., Cohen, D.L., Kuznetsov, S.A. & Langford, G.M. *J. Cell Sci.* **111**, 3221–3234 (1998).
- Hodge, T. & Cope, M.J. *J. Cell Sci.* **113**, 3353–3354 (2000).
- Mehta, A.D. *et al.* *Nature* **400**, 590–593 (1999).
- Rief, M. *et al.* *Proc. Natl. Acad. Sci. USA* **97**, 9482–9486 (2000).
- Sakamoto, T., Amitani, I., Yokota, E. & Ando, T. *Biochem. Biophys. Res. Commun.* **272**, 586–590 (2000).
- Rock, R.S. *et al.* *Proc. Natl. Acad. Sci. USA* **98**, 13655–13659 (2001).
- Walker, M.L. *et al.* *Nature* **405**, 804–807 (2000).
- Harada, Y. *et al.* *Nature* **409**, 113–115 (2001).
- Tanaka, H. *et al.* *Nature* **415**, 192–195 (2002).
- Yasuda, R., Miyata, H. & Kinosita, K. Jr. *J. Mol. Biol.* **263**, 227–236 (1996).
- Yamada, T. *et al.* *Biophys. J.* **80**, 80a (2001).
- Nishizaka, T., Yagi, T., Tanaka, Y. & Ishiwata, S. *Nature* **361**, 269–271 (1993).
- Suzuki, N., Miyata, H., Ishiwata, S. & Kinosita, K. Jr. *Biophys. J.* **70**, 401–408 (1996).
- Yasuda, R., Noji, H., Kinosita, K. Jr & Yoshida, M. *Cell* **93**, 1117–1124 (1998).
- Homsher, E., Wang, F. & Sellers, J.R. *Am. J. Physiol.* **262**, 714–723 (1992).
- Gelles, J., Schnapp, B.J. & Sheetz, M.P. *Nature* **331**, 450–453 (1988).
- Moore, J.R., Kremmentsova, E.B., Trybus, K.M. & Warsaw, D.M. *J. Cell Biol.* **155**, 625–635 (2001).
- Veigel, C., Wang, F., Bartoo, M.L., Sellers, J.R. & Molloy, J.E. *Nature Cell Biol.* **4**, 59–65 (2002).
- Howard, J. *Annu. Rev. Physiol.* **58**, 703–729 (1996).
- Hua, W., Chung, J. & Gelles, J. *Science* **295**, 844–848 (2002).
- Nishikawa, S. *et al.* *Biochem. Biophys. Res. Commun.* **290**, 311–317 (2002).
- Rice, S. *et al.* *Nature* **402**, 778–784 (1999).
- Cheney, R.E. *Methods Enzymol.* **298**, 3–18 (1998).
- Noji, H., Yasuda, R., Yoshida, M. & Kinosita, K. Jr. *Nature* **386**, 299–302 (1997).
- Miyata, H. *et al.* *Biophys. J.* **68**, 2865–290s (1995).
- Harada, Y. *et al.* *Biophys. J.* **76**, 709–715 (1999).
- Block, S.M., Goldstein, L.S. & Schnapp, B.J. *Nature* **348**, 348–352 (1990).